SCA2003-15

DEPRESSURIZATION UNDER TERTIARY CONDITIONS IN THE NEAR-WELLBORE REGION: EXPERIMENTS, VISUALIZATION AND RADIAL FLOW SIMULATIONS

P. Egermann, S. Banini and O. Vizika
Institut Français du Pétrole (IFP)

ABSTRACT

Depressurization can be a very interesting process to recover hydrocarbons from waterflooded oil reservoir with high gas-oil-ratio. Most of the published results are related to depletion experiments under secondary conditions (virgin reservoir). Data are more scarce under tertiary conditions after waterflooding [1, 2, 3].

The present paper treats the issue of the depressurization under tertiary conditions in the near-wellbore region. Practically, this has been achieved by combining experimental results, obtained on both core and transparent micromodel, with radial flow depletion simulations that are representative of the conditions prevailing in the near-wellbore region. A validated methodology previously presented [4] has been used to design the experiments on core (the core under tertiary conditions was continuously flushed with water at a fixed rate, while the pressure at the outlet was decreased to reproduce a drawdown). The saturation profiles, the pressures and the fluid productions as a function of time were recorded in the two experiments that are presented. From the core experiments, critical gas saturation (Sgc) and relative permeability (kr) have been determined using a specific simulation code that takes into account nucleation, diffusion and mobilization processes related to the appearance of the gas phase from solution. Constant depletion rate experiments were also conducted on a transparent micromodel to study the process of connection of the gas phase under tertiary conditions. The specificity of the near-wellbore region (high dP/dt and radial flow) was then investigated by conducting a numerical experiment with radial geometry.

It is shown that gas relative permeabilities obtained under tertiary conditions are lower than the ones obtained under secondary conditions. This behavior is attributed to the double connection process that is needed for the gas to get mobilized: connection of the disconnected oil phase and connection of the gas phase itself. This phenomenon is also confirmed by the visualization experiments conducted on micromodel. The numerical experiment representative of the near-wellbore conditions with a radial geometry demonstrates that Sgc is a function of the distance to the wellbore, which can have a large impact on reservoir simulation results.

INTRODUCTION

Depressurization under tertiary conditions is considered as an interesting process to extend economically the life of mature waterflooded reservoirs [5, 6]. The success of the process is mainly dependent on the recoverable fraction of the solution gas contained in the trapped oil and on the quantity of incremental oil that is possible to produce consecutively to the development of the gas phase [7].

Realistic estimations of this tertiary recovery can only be achieved with relevant values of both Sgc (critical gas saturation) and kr (relative permeability). Unfortunately, most of the published data on depressurization are related to depletion experiments under secondary conditions and are mainly focused on the evolution of the Sgc value as a function of the

depletion rate (dP/dt). Secondary depressurization has been looked at with coreflood experiments [8, 9, 10], with pore network modeling [11], or with visualization on transparent micromodel [12, 13]. The available results prove that krg values under internal gas drive are very low even at significant Sg values. This trend was observed for both light and heavy oils [14, 15]. More recently, it has been shown that internal gas drive krg values can be several orders of magnitude lower than the external gas drive krg [4, 16].

Data are more scarce on tertiary depressurization process. Lighthelm et al. [1] have mainly studied the evolution of Sgc as a function of dP/dt using cores and fluids from the Brent field. They showed that Sgc increases with dP/dt (same trend as under secondary conditions), but the Sgc value depends on the initial saturation state for a given core and a given set of fluids. The connection process of the gas phase under tertiary conditions was also studied in micromodel by Hawes et al. [17]. Only Grattoni et al. and Naylor et al. [2, 3] tackled simultaneously the issues of Sgc and kr under tertiary conditions. Grattoni et al. [2, 18] conducted depletion experiments on a model porous medium composed of transparent packed beads that enabled also flow visualization. The main result of this study is the extremely low values of krg measured, which were found around 10^{-5}-10^{-3} even at 23% Sg. This particular behavior was attributed to the intermittent flow of gas that was observed experimentally during the depletion process. Naylor et al. [3] conducted several depletion experiments at different rates on real aged cores. The krg curves were obtained by numerical history matching taking into account the specific shape of the local Sg profiles. The results obtained were in good agreement with the existing literature. Sgc increases with dP/dt and krg values are extremely low, around 10^{-4}.

In this paper, we will focus on the tertiary depressurization in the near-wellbore region. This part of the reservoir is particularly important for hydrocarbon production because it controls the well productivity / injectivity, whereas the far field region accounts for the overall recovery. Most of the published depressurization experiments are conducted at a fixed dP/dt, so that the pressure drop along the core remains moderate, even at high dP/dt. This makes this kind of experiments only representative of the far field region. In the first part of the paper, we present two coreflood experiments using a specific design and methodology that enables to reproduce the conditions that prevail in the near wellbore region [4]: high pressure gradient. The experimental results are interpreted using a tertiary depletion simulator. The related kr curves are presented and compared with other published results. The gas mobilization process under tertiary conditions is studied in the second part using visualizations obtained from a high pressure micromodel. In the third and last part, the specificity of the near-wellbore region is investigated by performing numerical experiments with a radial geometry to evaluate how the flowing properties vary as a function of the distance from the well.

CORE EXPERIMENTS

Rock/fluid system

All the experiments were performed on a Vosges sandstone core, whose main properties are gathered in Table 1. This choice was mainly motivated by the high degree of homogeneity of this sandstone and also by its fair absolute permeability.

Table 1: Vosges sandstone core properties

Permeability mD	Porosity %	Length cm	Area cm^2	PV cm^3
58	24	34.5	14.5	120

The same binary mixture C1C7 was used for the oleic phase in both experiments. The bubble point of the mixture was equal to 21 bar, which corresponds to a molar fraction of C1 equal to 0.107. The table hereafter provides the associated properties in terms of IFT and viscosity at Pb and 20°C. Data were derived from IFP developed PVT software.

Table 2: fluid properties of the binary mixture C1C7

Pb bar	% C1 molar	IFT mN/m	Oil viscosity cP	Oil density kg/m^3
21	10.7	17.25	0.402	672

The brine is composed of 50 g/l NaCl and 5 g/l $CaCl_2$. This composition proved to be efficient in stabilizing clays contained in the sandstone and in getting a good contrast between the oil and the water phase during the acquisition of local saturation measurements.

Experimental set-up

It is mainly composed of a Hassler type core holder made with composite material, which enables acquisition of local saturation measurements along the core with CT-scanner. In the inlet, the binary mixture or the brine can be injected into the core at a fixed rate with a pump. Downstream, the outlet pressure is controlled by a back pressure valve remotely operated by a PC, so that the drawdown can be monitored very easily. At the outlet, a densimeter is used mainly during the core preparation to check the core saturation with the mixture. During the experiment, the densimeter is also useful to detect the very first apparition of the gas phase downstream. Fluids are collected into a separator so that both liquids and gas quantities can be measured. Evolution of the outlet pressure is directly recorded by a pressure gauge. The inlet pressure is deduced from a differential pressure gauge measurement. Only the total pressure drop along the core is available (no pressure ports). All the data are automatically recorded on a PC.

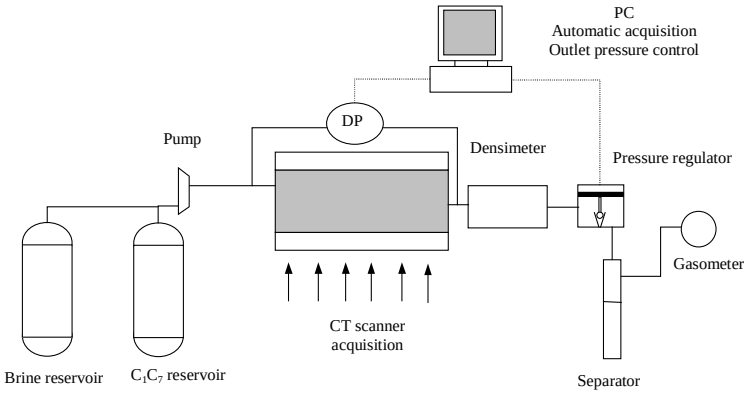

Figure 1 : coreflood experimental set-up

Experimental procedure

Residual oil saturation (tertiary conditions) was established with the following procedure:

- Preliminary setting of S_{wi} conditions using a viscous oil (Marcol 52, 10 cP)

- ü Miscible flooding of Marcol by C7
- ü Miscible flooding of C7 by the binary mixture C1C7 under pressure (above Pb)
- ü Setting of Sorw by injection of brine at fixed rate

The principle of the depletion experiment is described in earlier publication [4]. Under tertiary conditions, the brine is injected upstream at a fixed rate with the outlet pressure originally above the bubble point. Pressure at the outlet is progressively decreased down to a defined value below the bubble point of the mixture. All the experiments were performed with a rate of 30 cc/h to simulate conditions in the wellbore of a production well. The drawdown caused the formation of the gas phase starting in the downstream part of the core. Transient evolution of gas saturation through the core is followed by CT-scanner and impact of gas apparition on the pressure drop is detected on the inlet pressure variations.

Production data results

Two experiments were conducted (M1 and M2). The outlet pressure was decreased below the bubble pressure in two steps (17 and 14 bar) in the first experiment, whereas it was decreased directly down to 14 bar in the second experiment. For both experiments, the pressure evolutions are very similar and also in good agreement with previous experiments performed under secondary conditions (Figure 2). At the beginning, the inlet and outlet pressures remain parallel. This part corresponds to a constant pressure drop along the core during the flow of water when the outlet pressure is above the bubble point (residual oil immobile). As soon as the gas appears downstream, the pressure drop increases with increasing gas saturation, and then it stabilizes, while the outlet pressure is maintained constant (17 or 14 bar). The experimental results are summarized in Table 3.

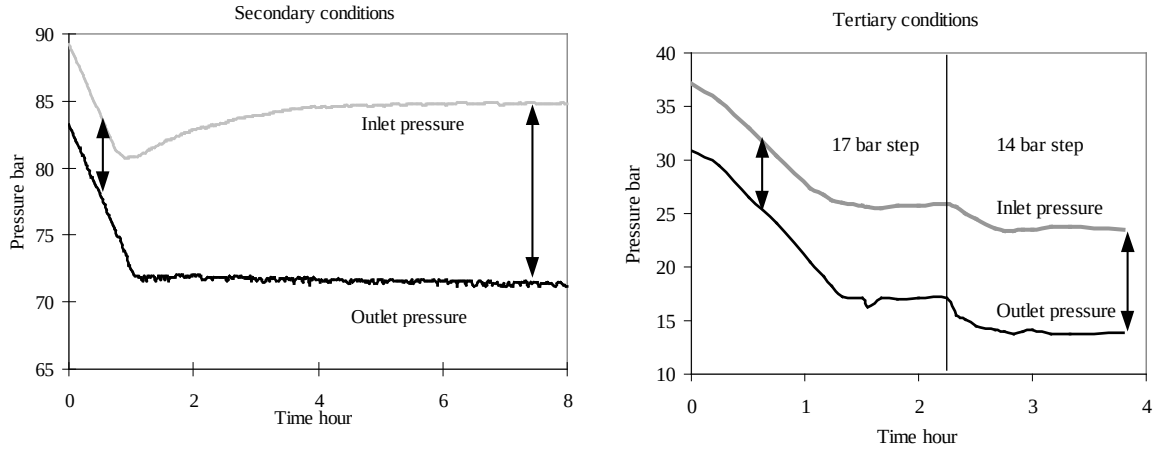

Figure 2 : inlet and outlet pressure evolutions (secondary conditions and M1)

One interesting feature concerns the evolution of the inlet pressure. A rebound was measured under secondary conditions and was associated to a recompression along the core consecutively to the development of the gas phase and its effect on kro (the oil was the injected fluid). The inlet pressure only decreases or stabilizes under tertiary conditions. This result suggests that the development of the gas phase has a less pronounced effect on the permeability of the injected fluid (krw). This may be a consequence of the tertiary conditions, where the gas appears within the oil phase, which is non mobile and trapped in the large pores since the rock is water-wet.

Table 3 : tertiary depletion experiments results

Exp	Sorw %	DP water / oil	Step1 / DP1	Step2 / DP2	Krw at Sorw	ΔSo %OOIP
M1	28.1	6.1 bar	17 bar / 8.7 bar	14 bar / 9.8 bar	0.057	42
M2	29.0	6.4 bar	14 bar / 9.1 bar		0.054	35

Figure 3 shows the evolution of the differential pressure and the incremental oil production as a function of time. In both experiments, the appearance of the gas phase makes the pressure drop along the core increase, and is associated with the production of a significant quantity of oil, which represents around 10% PV (34-42 % OOIP). In the two step experiment (M1), the break in the slope of the oil production curve strongly suggests that this incremental oil production is directly connected with the extension of the three-phase area into the core.

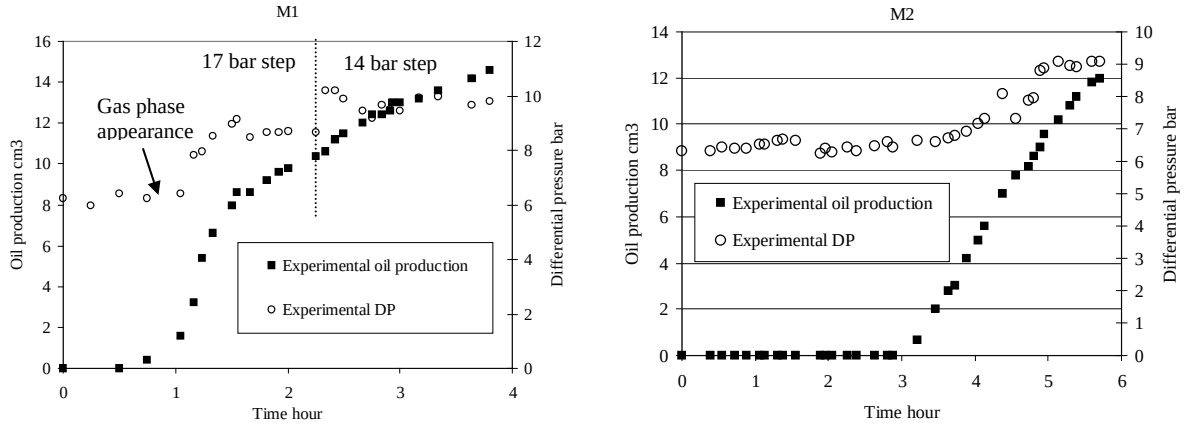

Figure 3 : Experimental pressure drop and oil production (M1 and M2)

Saturation profiles results

The above observations made on the production data are completely confirmed by the in-situ saturation measurements. Figure 4a illustrates the extension of the gas region upstream depending on the outlet pressure value (17 and 14 bar). The shape of the Sg profiles is very typical with a gas saturation jump ahead the gas region followed by a less pronounced increase of Sg. This shape was found common in all experiments and very similar with the results obtained under secondary conditions [4].

Another interesting feature concerns the evolution of the Sw profiles during M1 (Figure 4b). The Sw value remains very uniform and constant within the three-phase area suggesting that the non wetting phase saturation (Sg+So) value is around 35%, close to the original Sorw value, whatever the experimental conditions.

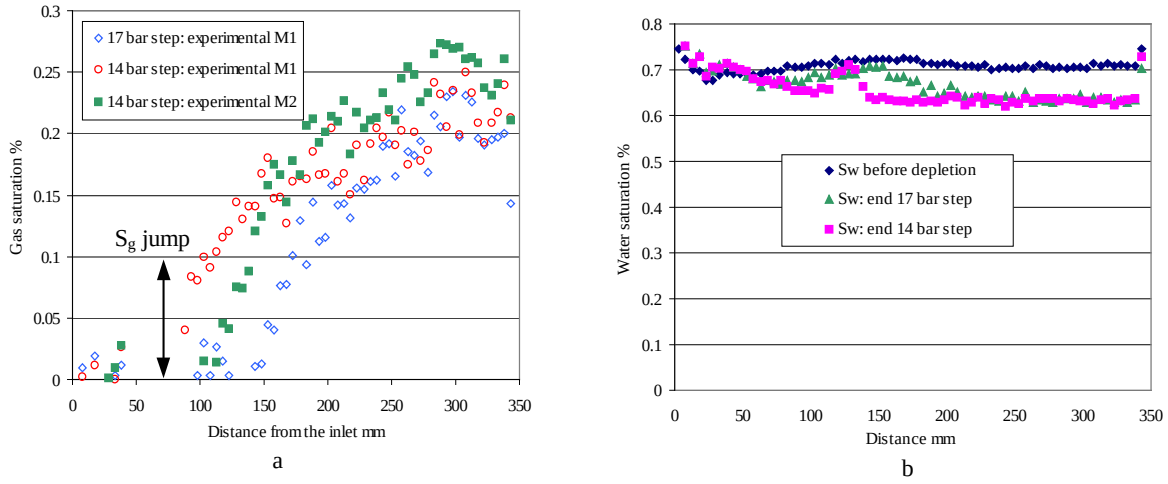

Figure 4 : (a) Sg profiles (M1 and M2) ; (b) Sw profiles M1

The conservation of the overall non-wetting phase saturation also explains why the development of the gas phase has a less pronounced impact on the inlet pressure, and on the injected phase permeability than under secondary conditions.

Interpretation

Numerical simulator

The in-house depletion code that was developed to simulate the experiments under secondary conditions was used [19]. The general structure of the code is reminded in Figure 5. The main advantages of this code are listed below:

- ü Account of the physical phenomena involved in the gas formation (nucleation, diffusion)
- ü Control of the gas mobilization process. Depending on the experimental conditions, the code can handle both dispersed or continuous gas flow.

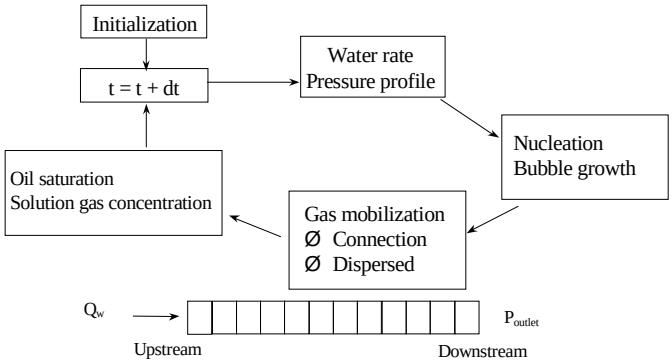

Figure 5 : code architecture

Some modifications have been introduced in the original code in order to take into account the specificity of the tertiary conditions.

- ü The pressure drop along the core results from the injection of the water phase (krw(Sg))
- ü The three-phase flow was handled like a pseudo two-phase flow. As the local saturation measurements showed that the non wetting phase saturation remains

constant within the three-phase region, the oil saturation in each cell was calculated from the gas saturation value using the conservation of the non wetting phase saturation:

$$So = S_{NWR} - Sg\,, \quad \text{where } S_{NWR} \text{ was kept constant and equal to 35\%}$$

History matching

A very good agreement was reached between the simulation and the experimental data in terms of production data and Sg profiles (Figure 6), whatever the value of the outlet pressure. The consistency of this history matching was also checked by comparing the experimental and the simulated gas production a posteriori. Here again, an excellent matching is obtained (Figure 7a).

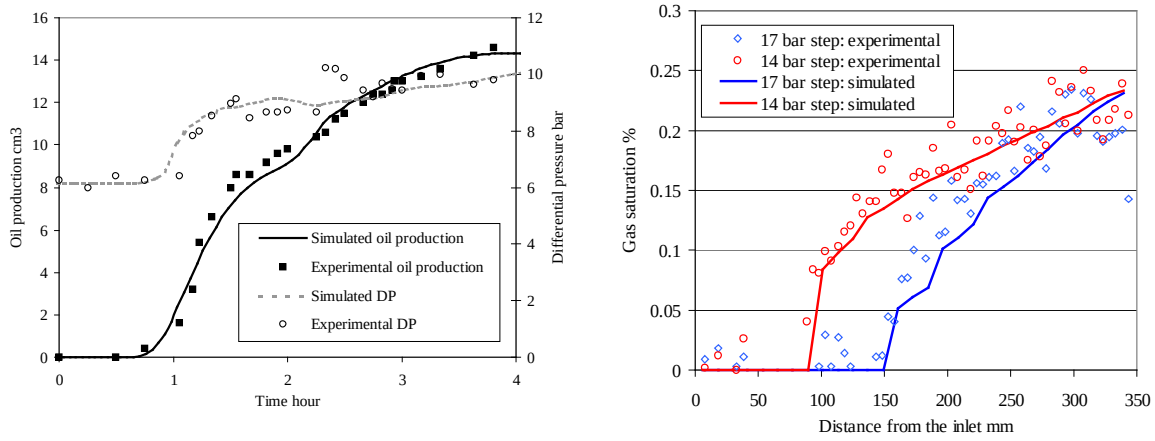

Figure 6 : history matching of M1 (production data and Sg profiles)

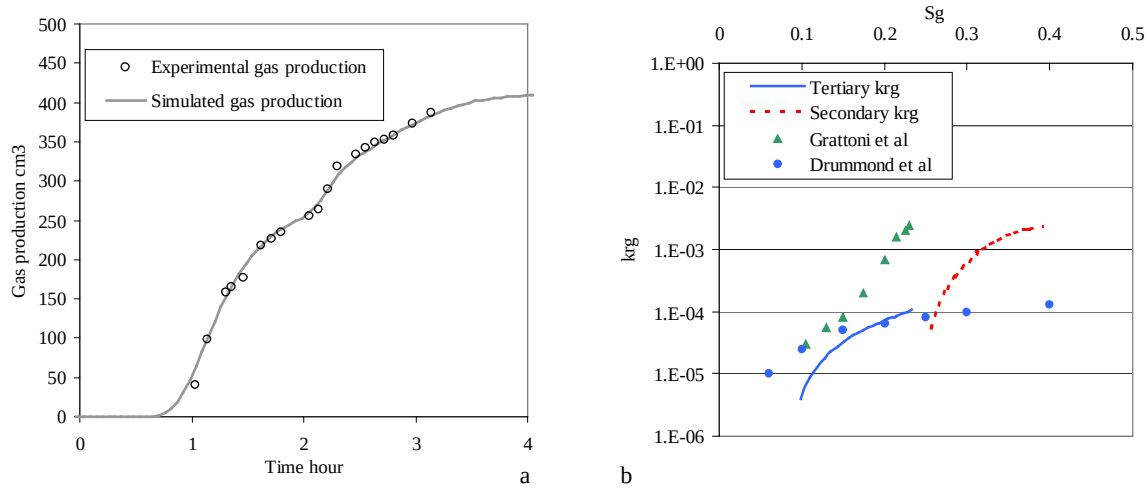

Figure 7 : gas production history matching (a) and krg results (b)

Krg curve shape

The tertiary krg curve deduced from the history matching procedure is compared with the secondary krg curve that was obtained on another rock sample in Figure 7b [4]. Both curves show that the mobility of the gas phase is limited under depletion, but this trend is more pronounced under tertiary conditions. It suggests that one part of the gas formed into the porous medium does not participate in the gas flow under tertiary conditions, which leads to a

lower krg value at a given Sg, comparing to the secondary conditions case. As the gas comes from solution within the trapped disconnected oil, it is suspected that the one part of the gas formed in non accessible oil ganglia can miss the connection process and explain this result. Although the experiments under tertiary and secondary conditions have not been conducted on the same rock, it is interesting to observe that a lower Sgc value is found under tertiary conditions for similar drawdown rate (even if krg are lower). This may be a consequence of the water wettability of the rock, which favors the entrapment of the oil phase in the largest pores. Hence, it makes the gas phase appears under tertiary conditions in the class of pores that accounts for the porous medium connectivity leading to lower Sgc value comparing to the secondary case, where the gas bubbles can be created in every classes of pores.

The tertiary krg curve is also in good agreement with the other available published results from Grattoni et al. [2] and Naylor et al. [3] (corresponding krg curve in Drummond et al. [6]). All curves have a common part around 10^{-4}, which confirms the gas mobility is very limited under tertiary conditions, whatever the experimental conditions.

VISUALIZATION EXPERIMENTS: GAS MOBILIZATION PROCESS

A pressurized micromodel was used to visualize the gas mobilization process under tertiary conditions and explain the low values of krg measured on coreflood experiments. The general principle of the experimental set-up is presented in Figure 8. The micromodel can be operated up to 100 bar and 60°C using a circulating device of the heated confining fluid. The establishment of the tertiary conditions with C1C7 was achieved using the procedure followed with coreflood experiments. The depletion was conducted at fixed depletion rate (dP/dt) by closing the inlet valve and decreasing progressively the pore pressure through the back pressure valve.

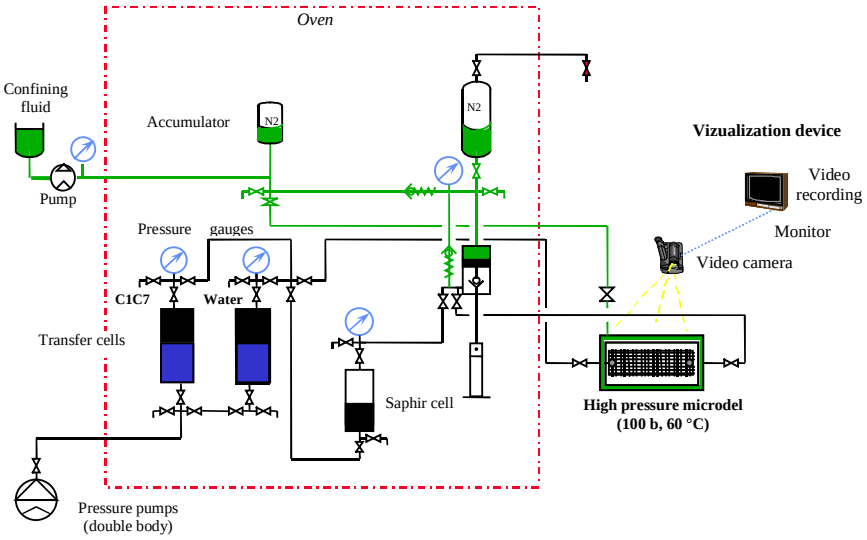

Figure 8 : Experimental set-up for Micromodel visualization

A sequence of the gas phase development is given in Figure 9. On the first picture, the gas bubbles (white) start appearing from the oil ganglia (blue) disconnected by the water phase (red). Depending on the size of the ganglia and the available quantity of solution gas in the vicinity of the bubbles, the growing rate can be very different from one bubble to another. Several connection events between two adjacent bubbles are also observed, whereas some bubbles remain disconnected during the whole experiment. At the end of the sequence, a large

gas bubble is obtained, whereas a significant fraction of the gas phase is still disconnected within the disconnected oil ganglia. From these observations, the low values of krg measured from coreflood experiments can be qualitatively explained by the double mechanism of connection needed for the gas to get mobilized: reconnection of the oil phase and connection of the gas itself. This mechanism is also very similar to what is observed under tertiary gravity assisted inert gas injection as shown by Kantzas et al. [20].

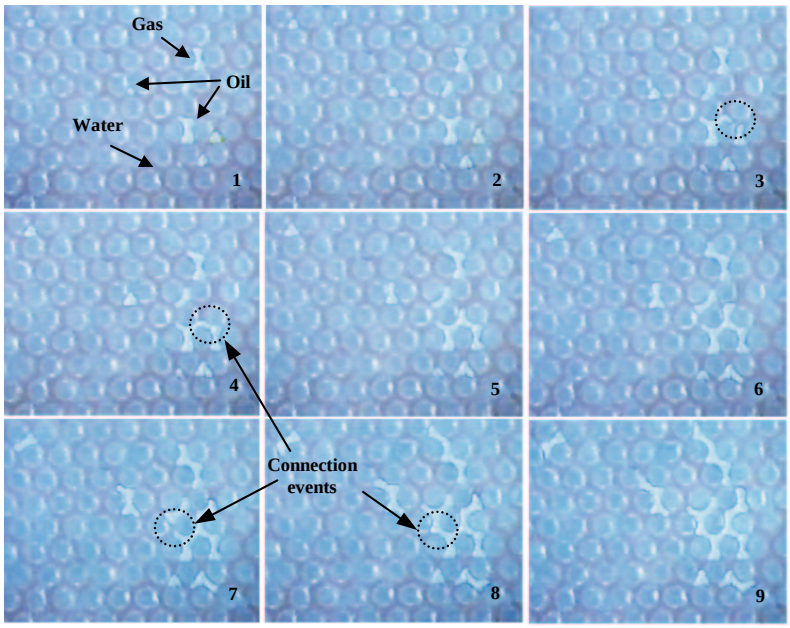

Figure 9 : Development of the gas phase under tertiary conditions

RADIAL GEOMETRY EFFECT IN THE NEAR WELLBORE

Principle

The near wellbore region is characterized by a high drawdown and radial geometry. The high drawdown is reproduced in our experiments by injection of the producing fluid at a sufficiently high rate, but the flow is linear, which makes the pressure gradient (dP/dx) uniform along the core. As the flow is radial near the well, both dP/dx and U (fluid velocity) increase from the far field to the near wellbore region, so the equivalent depletion rate dP/dt, equal to U×dP/dx, also increases [4]. As the flowing parameters (Sgc, kr) are strongly dependent on dP/dt, we have designed a numerical laboratory experiment with a radial geometry to investigate the evolution of the flowing properties as a function of the distance from the well.

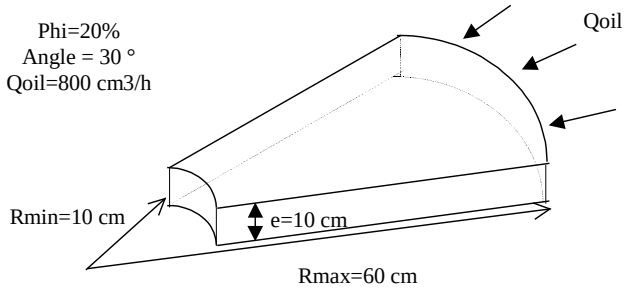

Figure 10 : principle of the radial numerical experiment

The simulations were performed under secondary conditions. The numerical experiment principle is shown in Figure 10 and is the same as the one followed for the coreflood experiments. The depletion simulator was first calibrated on an existing experiment with a linear geometry to fix the parameters controlling the nucleation, the diffusion and the gas mobilization. It is worth reminding that our code enables to evaluate the local Sgc value from the bubble population properties (size, number) and a shape factor to take into account the bubble ramifications for connection criterium. After calibration, the code was slightly modified to handle radial geometry and the numerical experiment was launched.

Results

Figure 11 shows the pressure profiles with both geometries. As expected, the pressure gradient dP/dx increases near the outlet when a radial geometry is considered, whereas dP/dx remains uniform along the core with a linear geometry. The associated Sg profiles have a similar shape with a gas saturation jump followed by a less pronounced increase of Sg, whatever the geometry considered (Figure 12). The mobilization of the gas phase can be detected from the break in the slope of the Sg profiles (when the increase is less pronounced). With linear geometry, the break occurs always at the same saturation, whereas the break is clearly a function of the distance with radial geometry suggesting Sgc value varies from the outlet part of the core to the inlet.

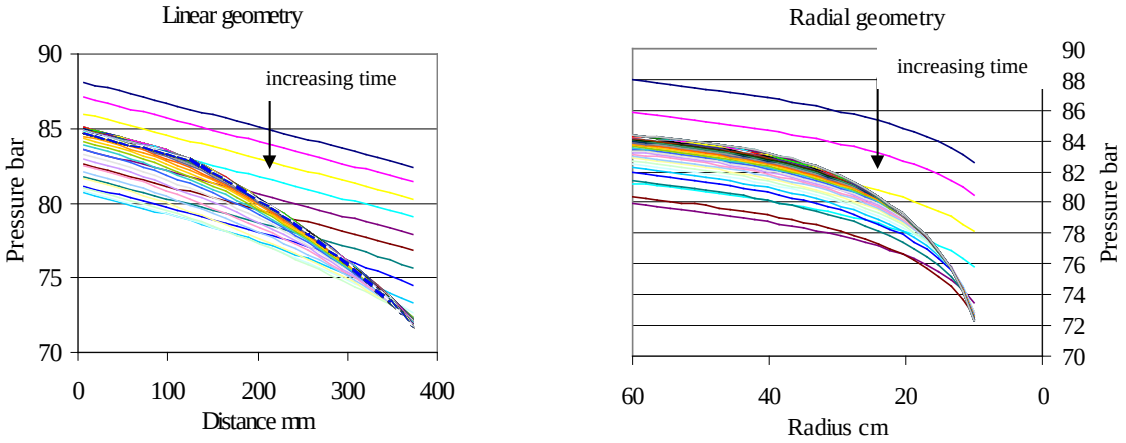

Figure 11 : pressure profiles with linear and radial geometry

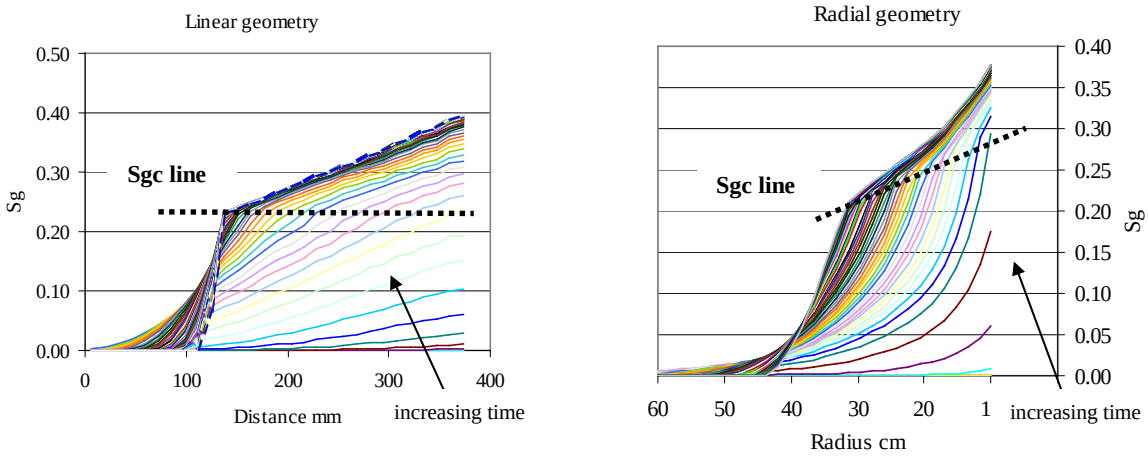

Figure 12 : Sg profiles with linear and radial geometry

This behavior is confirmed in Figure 13, where the Sgc values calculated by the code in each cell are plotted as a function of the distance. When a linear geometry is considered, the calculated Sgc values are very uniform along the core, equal to 24%, which is in line with the experimental data and the theory (high equivalent dP/dt is constant along the core, several meters away from the well).

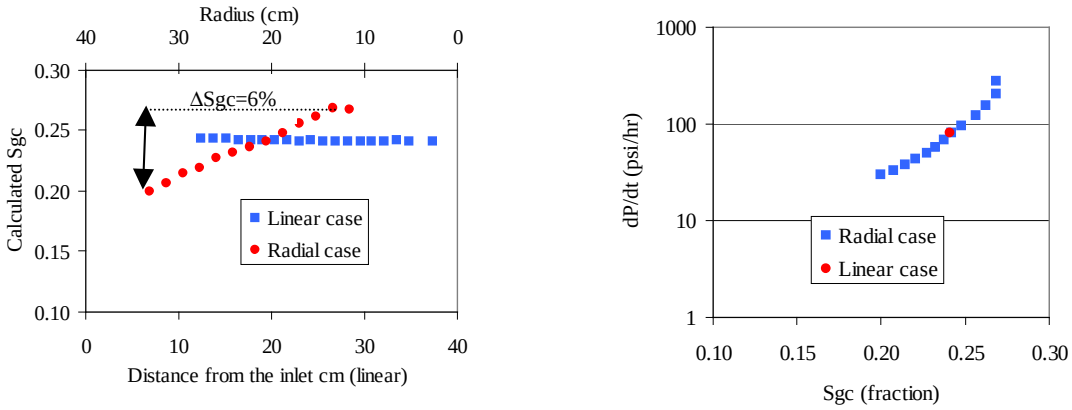

Figure 13 : calculated Sgc values along the core in linear and radial geometry

When a radial geometry is considered, the calculated Sgc value varies from 26% near the outlet, where the equivalent dP/dt is maximum, down to 20% at the gas front, where the dP/dt value is lower. The calculated Sgc values are clearly a function of dP/dt (Figure 13) and fall along a linear trend in semi-log scale as already pointed out by Scherpenisse et al. [9]. This study confirms the role played by the flow geometry in the spatial distribution of the flowing properties under depletion. When significant drawdown values are observed in the field (high production rates or heavy oil production) this dependence has limited effects on the overall field recovery [21] but may impact the production performances significantly and should be taken into account in reservoir simulations.

CONCLUSIONS

It is shown that the gas relative permeability curve obtained under tertiary conditions is lower than the one obtained under secondary conditions. This behavior is attributed to the double connection process that is needed for the gas to get mobilized: connection of the disconnected oil phase and connection of the gas phase itself. This phenomenon is also confirmed by the visualization experiments conducted on micromodel. The numerical experiment representative of the near-wellbore conditions with a radial geometry demonstrates that Sgc is a function of the distance, which can have large impact on reservoir simulation results.

ACKNOWLEDGEMENTS

This work was partly funded by ARTEP, a research association between TOTAL, ELF, Gaz de France and IFP.

NOMENCLATURE

dP/dt:	depletion rate	Pb:	bubble pressure
dP/dx:	pressure gradient	Q:	total injection rate
IFT:	interfacial tension	Si:	saturation of phase i
kri:	relative permeability of phase i	Sorw:	residual oil saturation to waterflood
OOIP:	oil originally in place	U:	fluid velocity

REFERENCES

1 Ligthelm D.J., Reijnen G.C.A.M. et al :'' Critical gas saturation during depressurisation and its importance in the Brent field'', SPE 38475, Offshore Europe Conference, 9-12 Sept 1997, Aberdeen.
2 Grattoni C.A. et al. :"Relative permeabilities for the production of solution gas from waterflood residual oil", SCA 9817, The Hague, 14-16 Sept 1998.
3 Naylor P. et al. :"Relative permeability measurement for post-waterflood depressurisation of the Miller field, North Sea", SPE 63148, ATCE, Dallas, 1-4 Oct 2000.
4 Egermann P. and Vizika O. :"A new method to determine critical gas saturation and relative permeability during depressurisation in the near-wellbore region", SCA 2000-36, Abu Dhabi, 18-22 Oct 2000 (published in Petrophysics, July-August 2001).
5 Braithwaite C.I.M., Schulte W.M. :'' Transforming the future of the Brent Field : Depressurisation-The next developpement phase'', SPE 25026, European Petroleum conference, 16-18 November 1992, Cannes.
6 Drummond A. et al. :"An evaluation of post-waterflood depressurisation of the Soth Brae field, North Sea", SPE 71487, ATCE, New Orleans, 30 Sept-3 Oct 2001.
7 Christiansen S.H., Wilson P.M., :'' Challenges in the Brent field : implementation of depressurisation'', SPE 38469, Offshore Europe Conference, 9-12 Sept 1997, Aberdeen.
8 Kortekaas T.F.M., Van Poelgeest F. :'' Liberation of solution gas during pressure depletion of virgin and watered-out oil reservoirs'', SPE 19693, ATCE, 8-11 Oct 1989, San Antonio.
9 Scherpenisse W., Wit K. et al :'' Predicting gas saturation buildup during depressurisation of a North Sea oil reservoir'', SPE 28842, European Petroleum Conference, 25-27 Oct 1994, London.
10 Kamath J., Boyer R.E. :"Critical gas saturation and supersaturation in low permeability rocks", SPE Formation Evaluation, pp 247-253, December 1995.
11 Du C., Yortsos Y.C. :''A numerical study of the critical gas saturation in a porous medium'', Transp porous media, V35, n°2, pp 205-225, May 1999.
12 Danesh A. et al. :"Pore level visual investigation of oil recovery by solution gas drive and gas injection", SPE 16956, ATCE, Dallas, 27-30 Sept 1987.
13 Bora R. et al. :"Flow vizualisation studies of solution gas drive process in heavy oil reservoirs with a glass micromodel", SPE Reservoir Evaluation and Engineering, pp 224-229, June 2000.
14 Tang G-Q., Firoozabadi A. :'' Gas and liquid phase relative permeabilities for cold production from heavy oil reservoirs'', SPE 56540 , ATCE, 3-6 Oct 1999.
15 Kumar R., Pooladi-Darvish M. :'' An investigation into enhanced recovery under solution gas drive in heavy oil reservoirs'', SPE 59336, IOR Symposium, Tulsa, 3-5 April 2000.
16 Poulsen S. et al. :"Network modelling of internal and external gas drive", SCA 2001-17, Edinburgh, UK, 17-19 Sept 2001.
17 Hawes R.I. et al. :"The release of solution gas from waterflood residual oil", SPE Journal, Volume 2, Dec 1997.
18 Grattoni C.A. and Dawe R.A. :"Gas and oil production from waterflood residual oil: effect of wettability and oil spreading characteristics", Wettability Conference, Tasmanie, 2002.
19 Egermann P. and Vizika O. :''Critical gas saturation and relative permeability during depressurisation in the far field and the near-wellbore region'', SPE 63149, ATCE, Dallas, 1-4 Oct 2000.
20 Kantzas A., Chatzis I., Dullien F.A.L. : '' Mechanisms of capillary displacement of residual oil by gravity-assisted inert gas injection'', SPE 17506, Rocky Mountain Regional Meeting, Casper, 11-13 May 1988.
21 Sahni A. et al. :'' Experiments and analysis of heavy oil solution gas drive'', SPE 71498, New Orleans, 30 Sept – 3 Oct 2001.